Temperature behaviour of iron nanograins in Nanoperm-type alloys

2003 J. Phys.: Condens. Matter 15 5637

(http://iopscience.iop.org/0953-8984/15/32/323)

INSTITUTE OF PHYSICS PUBLISHING JOURNAL OF PHYSICS: CONDENSED MATTER

J. Phys.: Condens. Matter **15** (2003) 5637–5648 PII: S0953-8984(03)61942-9

Temperature behaviour of iron nanograins in Nanoperm-type alloys

Marcel Miglierini[1] **and Jean-Marc Greneche**[2]

[1] Department of Nuclear Physics and Technology, Slovak University of Technology, Ilkovičova 3, 812 19 Bratislava, Slovakia
[2] Laboratoire de Physique de l'Etat Condensé, CNRS-UMR 6087, Université du Maine, 72085 Le Mans Cedex 9, France

Received 1 April 2003
Published 1 August 2003
Online at stacks.iop.org/JPhysCM/15/5637

Abstract

The evolution of hyperfine interactions with temperature is studied for $Fe_{80}M_7Cu_1B_{12}$ (M = Mo, Nb and Ti) nanocrystalline alloys with the help of ^{57}Fe Mössbauer spectrometry. The nanocrystalline structure features an amorphous residual matrix surrounding the crystalline nanograins of bcc-Fe. In addition, interfacial regions comprising atoms located on the surface of nanocrystals are considered. Special attention is paid to the temperature behaviour of hyperfine magnetic fields of the nanograins. The temperature dependence of hyperfine magnetic fields pointed out significant differences between bulk and nanosized bcc-Fe, suggesting a decrease in the corresponding magnetic ordering temperature. The higher the crystalline content is, the lower the difference between the hyperfine fields of bulk bcc-Fe and nanocrystalline Fe grains. This tendency is observed for M = Nb and Ti whereas it is completely opposite for M = Mo. The present results are explained in terms of mechanical stresses induced during the transformation from the amorphous to the nanocrystalline state, thus excluding a significant number of impurities diffused into the nanocrystalline grains.

1. Introduction

Technically attractive features of nanocrystalline alloys prepared by controlled annealing of amorphous precursors [1–3] are placing them into the centre of both technological and scientific perspectives. In particular, advantageous combination of magnetic parameters [4] leads to variety of practical applications [5]. In order to tailor the desired magnetic properties it is inevitable to understand the behaviour of magnetic interactions that are governed by (micro)structural characteristics. From a structural point of view, nanocrystalline alloys exhibit fine crystalline grains (grain size is typically about 7–20 nm) homogeneously scattered in the remaining amorphous matrix [6].

Such a two-phase system presents complex magnetic interactions subjected to fluctuations due to local arrangement of atoms and because the size of nanocrystalline grains is smaller than the ferromagnetic correlation length. Consequently, microscopic analytical techniques should be employed for their investigation. They usually aim to provide structural characterization with respect to the type, dimensions, shape and contents of nanocrystallites. A unique possibility to study simultaneously structural features and magnetic microstructure is offered by Mössbauer spectrometry.

In this paper, we present Mössbauer effect measurements performed under different conditions (temperature of annealing, temperature of measurement) upon Nanoperm-type $Fe_{80}M_7Cu_1B_{12}$ nanocrystalline alloys (M = Mo, Nb, Ti). They are characterized by the presence of bcc-Fe crystalline phase. Because iron is principally suited for Mössbauer spectrometry more detailed insight into the local atomic arrangement was envisaged. We also performed x-ray diffraction (XRD) measurements that confirmed the presence of bcc Fe. Due to the complexity of the XRD patterns of these systems, especially those with rather low or high crystalline fraction, it remains difficult to estimate accurately the lattice parameter of the crystalline phase. Consequently, no correlation was clearly found as far as lattice parameter is concerned.

The reason for choosing the system studied was twofold.

(i) The vast majority of papers devoted to Nanoperm-type alloys deals with the FeZr(Cu)B system. Thus, for the sake of generality we wanted to verify the behaviour of the crystalline phase for another material's composition.
(ii) Substituting miscellaneous metals for M, magnetic states of constituent atoms are modified in the amorphous phase as well as after nanocrystallization [7].

Different temperatures of annealing used have resulted in different relative contents of crystalline grains. In this way we have obtained a variety of magnetic arrangements which allowed the diversity of hyperfine interactions to be inspected.

Our attention was focused on the temperature behaviour of hyperfine magnetic fields of the crystalline phase because these data are still missing in the literature. Only the results published for Fe–Zr–Cu–B alloys with different metalloid concentration [8, 9] and for $Fe_{92}Zr_8$ [10] referring to one particular heat treatment are available. More recently, $Fe_{86-x}Cu_1Nb_xB_{13}$ ($x = 4, 5, 7$) nanocrystalline alloys obtained under different annealing conditions were investigated with the help of Mössbauer spectrometry and magnetization measurements [11]. Using a novel approach to the fitting of Mössbauer spectra [12, 13] evidence for superparamagnetic behaviour at low nanograin concentrations was given. At higher nanograin concentrations the particle–particle interaction leads to a collective magnetic behaviour, i.e. by an external field induced super-ferromagnetism [11]. The temperature dependences of hyperfine field, particularly that of nanocrystalline grains, are discussed on the basis of structural features.

2. Experimental details

2.1. Characterization of the samples

Nanocrystalline alloys of the nominal composition of $Fe_{80}M_7Cu_1B_{12}$, M = Mo, Nb or Ti, were prepared from their amorphous counterparts by 1 h annealing in protective Ar atmosphere. Details on preparation of the as-quenched and the nanocrystalline specimens were reported elsewhere [14]. Structural and magnetic characterization including differential scanning calorimetry (DSC), XRD, transmission electron microscopy (TEM), scanning tunnelling

microscopy (STM) and conventional magnetic measurements along with room temperature Mössbauer effect studies can be found in [7].

Mössbauer spectra were taken by a conventional constant acceleration apparatus working in transmission geometry with a ^{57}Co(Rh) source. Samples, which were placed in a cryofurnace operating between 77 and 673 K, consisted of a set of ribbons maintained by means of a single adhesive tape, to avoid thus mechanical stresses when cooling the sample to low temperature. The upper limit of the measuring temperature was chosen according to the particular sample measured and it was always at least 50° below the onset of crystallization determined from DSC curves. Possible temperature induced structural changes were carefully checked by recording spectra at room temperature after each temperature cycle. The temperature dependence of hyperfine fields of the bulk bcc-Fe was taken from the work of Preston *et al* [15]. However, calibration bcc-Fe foil was measured at several temperatures and the obtained spectral parameters were compared with the former. They are consistent with the previous ones within the error bar due to the small temperature deviation (about 2 K).

2.2. Fitting model

Besides a broad spectral component of the amorphous matrix and a narrow one of the bcc-Fe nanocrystals, a third component must be used in order to obtain a satisfactory fit to the experimental data. Its presence is not doubted and it is generally accepted. Its existence is justified from structural assumptions though it is still a point of controversy in the literature. It is usually refined by the help of a broadened sextet [8, 9, 16, 17] or a distribution of hyperfine fields [18, 19]. Sometimes it is included in one distributed spectral component which extends over the whole range of magnetic hyperfine fields [20, 21].

Mössbauer spectra were evaluated according to the fitting procedure whose basic features were described earlier [22, 23]. It consists of two independent blocks of distributed components and one sextet assigned to the bcc crystalline phase. One of the distributions is a distribution of hyperfine magnetic fields $P(B)$ which reconstructs the spectral component localized in the inner side of the narrow sextet. In some spectra with hardly visible crystalline contribution this distributed component is eventually omitted.

Unlike the case in the original fitting method [22], here we are introducing constraints on line intensities of individual sextets. All magnetically split components (distributions and a crystalline sextet) have the same line intensity ratio within one particular spectrum as proposed by Suzuki and Cadogan [24]. This parameter was, however, refined for individual spectra taken at different temperatures. Limitations were also applied as far as the maximal value of hyperfine fields belonging to the distributed components is concerned. All B-values are smaller than the hyperfine magnetic field of the crystalline component. The latter is, of course, a fitted parameter. Relative areas of all components were free in the fit. But great attention was given to ensure a physical temperature dependence of the different hyperfine parameters.

The fitting scheme described above was realized independently by means of NORMOS [25] and MOSFIT [26] programs.

3. Results

The amorphous precursor of the $Fe_{80}M_7Cu_1B_{12}$ alloy depicts interesting magnetic behaviour. Choosing M = Mo, Nb and Ti, the resulting magnetic ordering temperature of the as-quenched samples is $T_C^{AM} = 265$, 333 and 412 K, correspondingly [7]. It gives thus a hierarchy for magnetic interactions in those systems as a function of M. The higher the Curie temperature the stronger are the magnetic interactions. Consequently, the magnetic arrangement at room temperature varies from entirely paramagnetic (M = Mo), through weak ferromagnetic

(M = Nb) up to a well developed ferromagnetic (M = Ti) ordering. Annealing at different temperatures has provided diverse amounts of bcc-Fe nanocrystalline grains. Characterization of the magnetic microstructure at room temperature was recently performed by the help of several methods (XRD, DSC, TEM, STM, Mössbauer and magnetic measurements) [7]. In addition, the bulk and surface of the same samples were compared using transmission and conversion electron Mössbauer spectrometry [27]. The focus was put more on the behaviour of the intergranular phase.

In the following, we concentrate on some typical examples of the FeMCuB alloy with appropriate content of crystallites that enables the diversity of magnetic microstructure to be documented over a wide range of measuring temperatures with special emphasis on the crystalline phase. It is noteworthy that most research groups give attention to (predominantly Zr-containing) nanocrystalline alloys annealed behind the first crystallization (i.e. with considerable numbers of crystalline nanograins) that exhibit the best macroscopic magnetic parameters. On the other hand, mutual effects between the amorphous residual and the crystalline phases remain in most instances hidden.

Before introducing Mössbauer spectra of particular alloys we would like to make a general comment. In the figures, we present also individual subspectra that comprise a narrow Lorentzian line assigned to the crystalline phase and two broad distributed components that reconstruct the amorphous residual matrix and the interface atoms [22]. Though there are some disputes related to the latter and though the subspectra are usually not drawn in the literature we are showing them to stress the complexity of hyperfine interactions that occur in the nanocrystalline alloys. The composition and the crystalline fraction as well as the measuring temperature cause the resulting magnetic microstructure to vary considerably between ferromagnetic and paramagnetic arrangement. This imposes strong burdens on the fitting model applied which has to take into consideration the diversity of hyperfine interactions present in the samples. Aiming to visualize the occurrence of non-magnetic and magnetic regions especially in the amorphous residuum we offer this opportunity to the reader.

Some examples of Mössbauer spectra for nanocrystalline alloys annealed at different temperatures of annealing T_a and taken at different temperatures of measurement T_m are illustrated in figures 1 and 2. In addition, their decomposition into subspectral components is also reported, as obtained by the fitting model mentioned in the section above.

The crystalline A_{CR}, interfacial A_{IF} and amorphous A_{AM} contents in terms of iron atoms are listed in table 1 for the different nanocrystalline alloys (M = Mo, Nb, Ti), assuming the same recoil free fraction for the three components. In addition, the values of isomer shift δ and hyperfine field B_{CR} of the crystalline grains are reported as obtained from liquid nitrogen temperature measurements.

As observed in figure 1, the contribution of paramagnetic regions to the resulting Mössbauer spectra of Nb nanocrystalline alloys is more pronounced and emerges at a lower temperature than in the case of the Ti-containing alloy. Concerning $Fe_{80}Mo_7Cu_1B_{12}$ alloys, the originally fully paramagnetic amorphous precursor [7] exhibits magnetic hyperfine interactions which have developed in the retained amorphous phase after annealing. As seen in figure 2(a), at $T_a = 410\,^{\circ}C$ when an intermediate crystalline fraction (A_{CR}) is formed they are clearly recognized at low T_m. On the other hand, magnetic regions in the amorphous remainder are nearly suppressed at high enough measuring temperatures (figure 2(a)) giving rise to nearly pure paramagnetic doublets in the central parts of spectra. At the same time, the narrow lines which correspond to the crystalline phase are well established at low T_m. As the measuring temperature is increasing, these spectral lines are becoming broader due to superparamagnetic fluctuations and relaxation effects. The same tendency is also observed for higher T_a, i.e. higher A_{CR}, in the Mo samples (figure 2(b)).

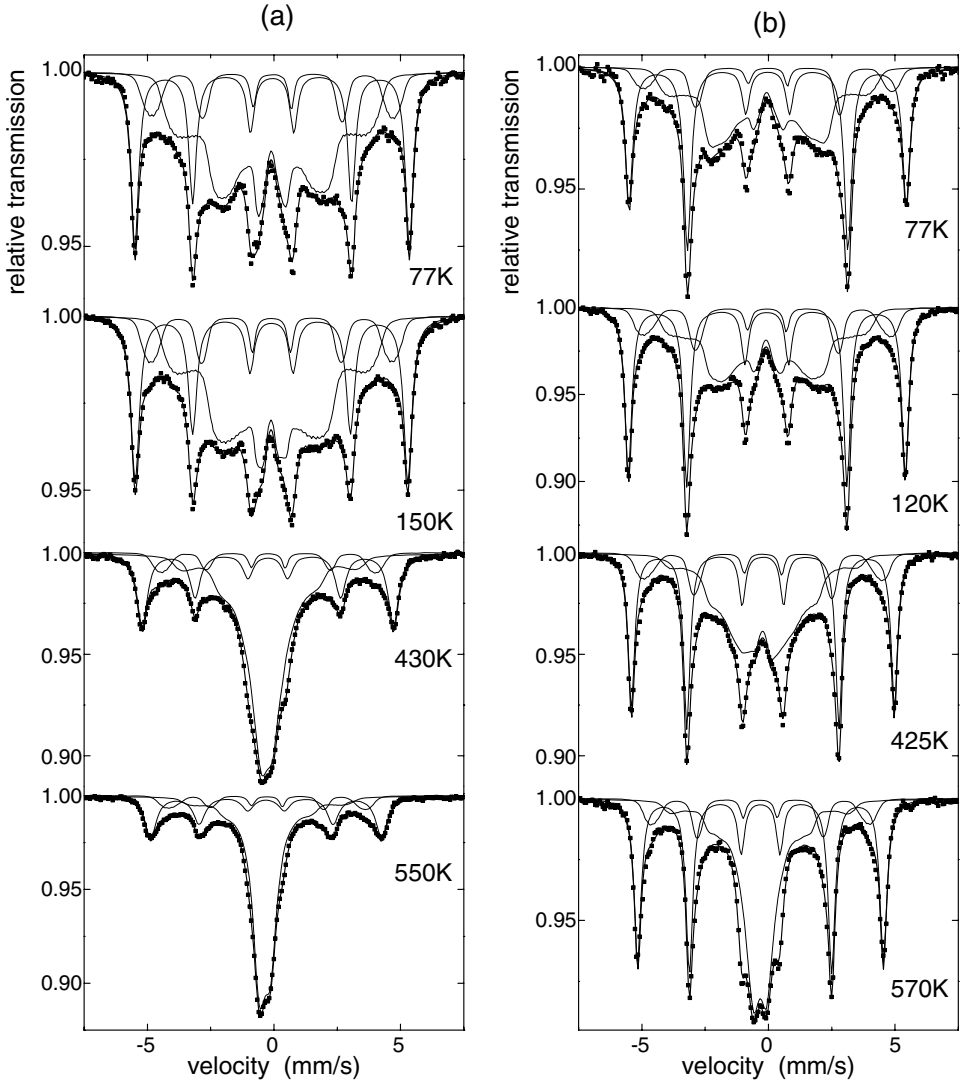

Figure 1. Mössbauer spectra taken at the indicated temperatures of nanocrystalline $Fe_{80}Nb_7Cu_1B_{12}$ (a) and $Fe_{80}Ti_7Cu_1B_{12}$ (b) obtained after 1 h annealing at 470 °C. Individual spectral components are also displayed.

Temperature dependences of hyperfine magnetic fields of the nanocrystalline and interfacial phase B_{hf} are plotted in figure 3 for all compositions studied. In accordance with the notation introduced in [28] we denote the crystalline fraction as low for A_{CR} ranging between 2 and 20%, intermediate (medium) for 20–50% and high for $A_{CR} > 50\%$. It should be noted here that for M = Nb the open circles in figure 3 represent an early stage of crystallization ($A_{CR} < 5\%$). The temperature evolutions of hyperfine field are compared to that of bulk bcc-Fe.

Even though the differences in hyperfine magnetic fields between bulk iron and nanocrystalline Fe grains are not very pronounced it should be stressed that they extend beyond the limits of possible error margin. Their determination cannot be questioned to depend

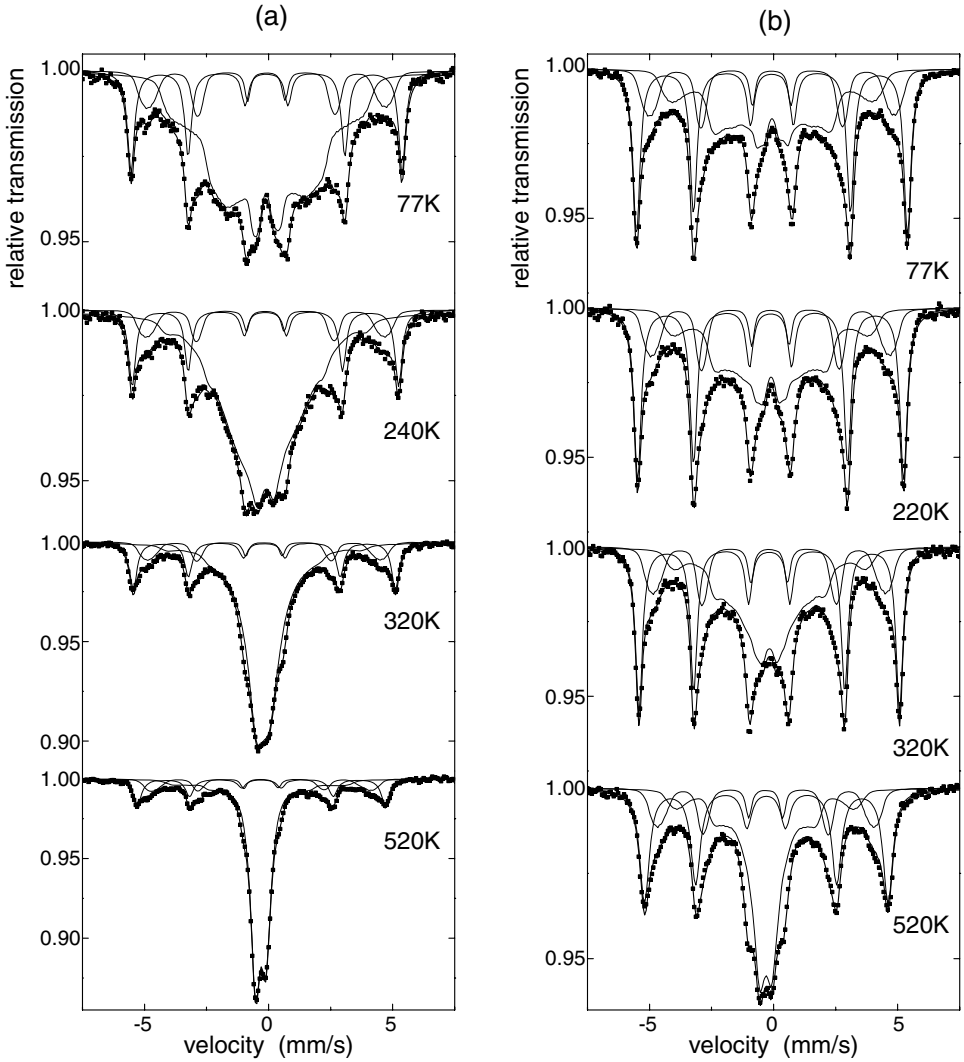

Figure 2. Mössbauer spectra taken at the indicated temperatures of nanocrystalline $Fe_{80}Mo_7Cu_1B_{12}$ obtained after 1 h annealing at 410 °C (a) and 470 °C (b). Individual spectral components are also displayed.

upon the fitting procedure applied. Figure 4 introduces Mössbauer spectra of nanocrystalline (nc-)$Fe_{80}Mo_7Cu_1B_{12}$ annealed at $T_a = 470$, 440 and 410 °C and taken at $T_m = 77$ K. The corresponding first Mössbauer lines are detailed on the right-hand panel. As clearly seen from the latter, the experimental points are reproduced with high reliability by narrow Lorentzian sextets, thus giving very accurate values of hyperfine fields assigned to the crystalline grains. One should concentrate especially on the outermost wings of the lines that are not so affected by the presence of other spectral components.

From figure 3(a), one observes different temperature dependences of hyperfine fields corresponding to nanocrystalline bcc-Fe in comparison to that of bulk bcc-Fe. In the case of nc-$Fe_{80}Nb_7Cu_1B_{12}$ they deviate towards low field values in the whole temperature range

Table 1. Characteristics, as a function of M element, of the amorphous precursor (Curie temperature T_C^{AM}) and the nanocrystalline $Fe_{80}M_7Cu_1B_{12}$ alloys (M = Mo, Nb and Ti) annealed at T_a: contents of iron atoms in the crystalline A_{CR}, interfacial A_{IF} and amorphous A_{AM} components (±5%), isomer shift δ (±0.02 mm s^{-1} quoted relative to metallic Fe at 300 K) and hyperfine field B_{CR} (±0.1 T) of the crystalline component at 77 K.

M	T_C^{AM} (K)	Parameter	T_a 420 °C	440 °C	470 °C	520 °C
		A_{CR} (%)	19	31	40	
		A_{IF} (%)	14	22	24	
Mo	265	A_{AM} (%)	67	47	36	
		δ (mm s^{-1})	0.08	0.11	0.11	
		B_{CR} (T)	33.9	34.3	33.7	
		A_{CR} (%)	2[a]	4	29	43
		A_{IF} (%)	—	2	17	20
Nb	333	A_{AM} (%)	98[a]	94	54	37
		δ (mm s^{-1})	0.01[a]	0.10	0.11	0.12
		B_{CR} (T)	32.9[a]	33.2	33.7	34.1
		A_{CR} (%)	12	28	41	
		A_{IF} (%)	6	12	12	
Ti	412	A_{AM} (%)	82	60	47	
		δ (mm s^{-1})	0.11	0.12	0.12	
		B_{CR} (T)	33.9	33.7	34.1	

[a] The temperature of annealing was 435 °C.

while the opposite tendency is evidenced for both Mo- and Ti-containing alloys in the low temperature range. At high temperature, the differences between hyperfine fields of bulk iron and nanosized Fe grains are growing with increasing temperature T_m for the three types of nanocrystalline alloy. Nevertheless, they are indirectly related to A_{CR} for M = Nb and Ti: the higher the crystalline content is, the lower the difference between the hyperfine field of the bulk and that of nanocrystalline Fe grains. The opposite behaviour is observed for the M = Mo alloy, however.

Temperature dependences of hyperfine fields corresponding to the interfacial phase depicted in figure 3(b) follow the same tendency as those of nanocrystalline bcc-Fe. Deviations between both curves of about 3 T are almost constant in the whole temperature range. This suggests a close similarity of resonant atoms which belong to the grains and to interfacial regions. Average values of hyperfine fields of the residual amorphous matrix are plotted as a function of measuring temperature in figure 5. Depending on the crystalline contents as well as on the composition of the master alloy, the temperature induced transformation from ferromagnetic to paramagnetic arrangement is accompanied by continuous reduction of the associated hyperfine fields. One observes that the higher the volumetric fraction, the higher the hyperfine fields at high temperature and the larger the effect of penetrating fields [28].

4. Discussion

Previous studies [8, 9] have discussed the high temperature dependence of the hyperfine field as a function of the volumetric crystalline fraction, taking into account magnetic interactions between grains and the amorphous remainder and magnetic behaviour of the latter. Low crystalline fraction suggests, at temperatures above the Curie point of the amorphous remainder, the presence of superparamagnetic fluctuations resulting from a magnetic

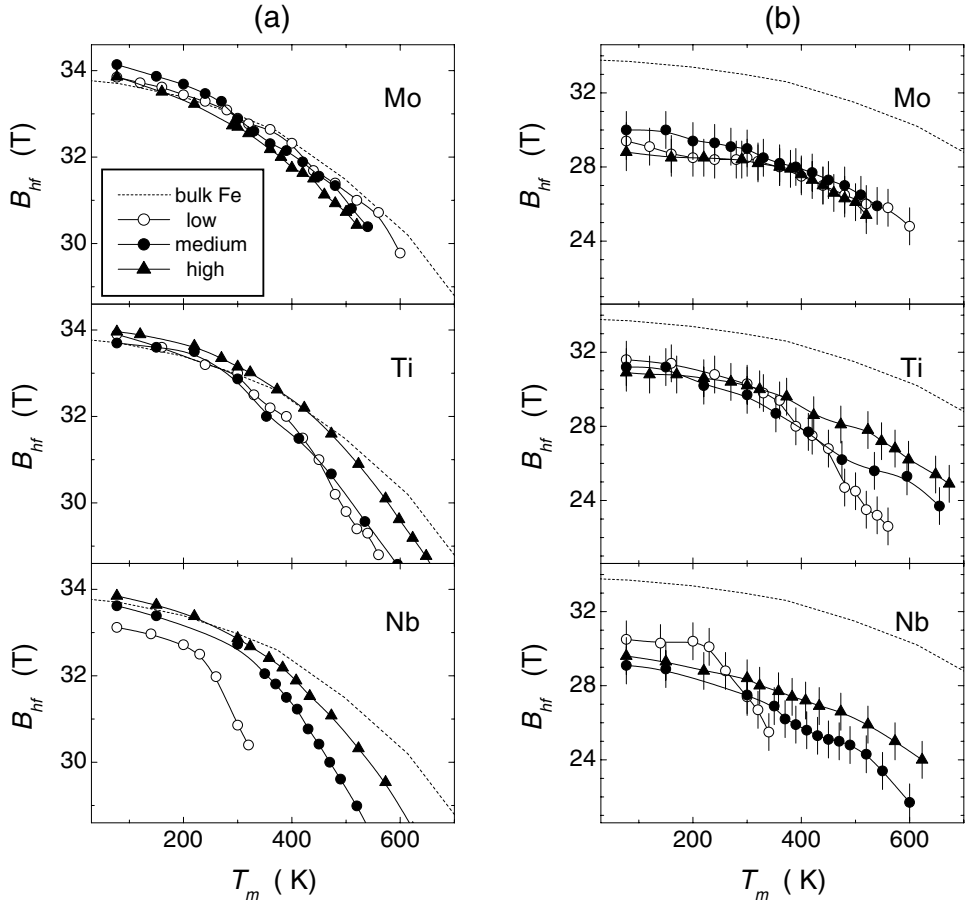

Figure 3. Hyperfine fields B_{hf} of the nanocrystalline bcc grains (a) and interfacial regions (b) versus temperature of measurement, T_{m}, for nanocrystalline $Fe_{80}M_7Cu_1B_{12}$ (M = Mo, Nb and Ti) with low, medium and high (see text) crystalline fraction. The dotted curve represents the temperature dependence of hyperfine fields for bulk iron.

decoupling between single domain grains embedded in a paramagnetic amorphous remainder. Thus such behaviour favours a decrease of the hyperfine field which is well observed for nc-$Fe_{80}Nb_7Cu_1B_{12}$ and nc-$Fe_{80}Ti_7Cu_1B_{12}$ alloys (see figure 3). An opposite tendency is revealed in nc-$Fe_{80}Mo_7Cu_1B_{12}$ alloys for which the lowest reduction is associated with the lowest volumetric crystalline fraction. In the case of both Nb and Mo systems, the presence of superparamagnetic fluctuations is undoubtedly evidenced by the broadening of the outer sextet and by a rapid emergence of a quadrupolar doublet, as shown in figures 1(a) and 2(a), respectively. Similar results were reports also in [11, 12]. When the volumetric crystalline fraction increases, the system progressively behaves as an interacting assembly of single-domain magnetic grains, i.e. the hyperfine field of Fe located in crystalline grains does strictly follow the same temperature dependence as that of bulk bcc-Fe.

Low temperature behaviour of FeZrBCu nanocrystalline alloys was previously discussed in terms of crystalline content with the presence of impurities located inside crystalline grains [9]. The combination of both B and Zr as impurity neighbour in the first two coordination

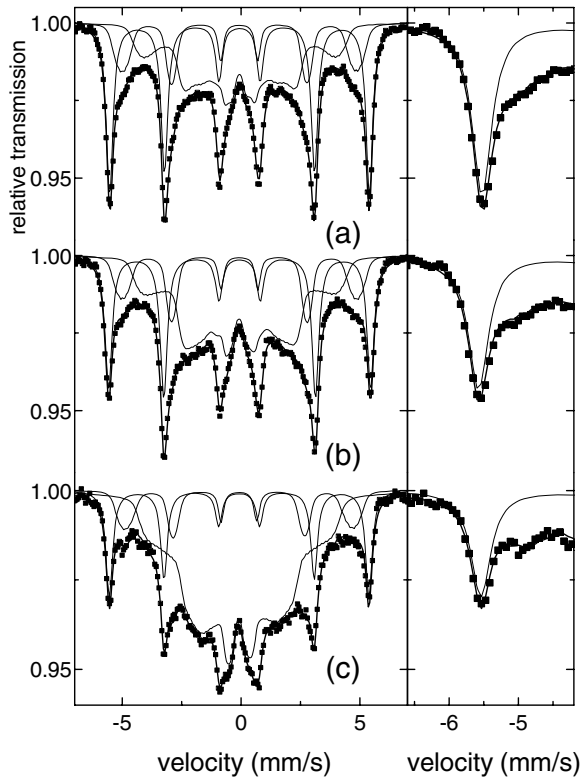

Figure 4. Mössbauer spectra (including spectral components) taken at 77 K of nanocrystalline $Fe_{80}Mo_7Cu_1B_{12}$ obtained after 1 h annealing at 470 °C (a), 440 °C (b) and 410 °C (c). The right panel shows expanded first Mössbauer lines.

shells was suggested to describe the hyperfine parameters. As an example, temperature dependences of hyperfine magnetic fields of bcc nanocrystalline grains were reported by Kemény *et al* for $Fe_{80}Zr_7B_{12}Cu$ [8] as well as for $Fe_{92-x}B_xZr_7Cu_1$ ($2 \leqslant x \leqslant 23$) [9] nanocrystalline alloys obtained by annealing of the amorphous precursors at 900 K and at the end of the first crystallization step, respectively. They observed faster decrease of the hyperfine field value of the main spectral component than the hyperfine field of pure bcc-Fe. In the latter case, a composition dependent decrease was observed, especially at higher temperatures. The mechanism responsible for the above mentioned effects is suggested to be the presence of 2–4 at.% Zr and B dissolved in the bcc phase, also causing modifications of Curie temperature [9].

In the present case, one unambiguously observes an increase of hyperfine field which remains quite high in the case of Mo-nanocrystalline alloys (figure 3) even though a decrease would be expected in agreement with the lowest Curie temperature of the amorphous precursor. The situation is less pronounced in the case of Ti and Nb samples for which an increase of hyperfine field is only observed at high volumetric crystalline fraction. Taking the explanations proposed in [8, 9] into account, such behaviour would indicate lower impurity contents for high A_{CR} which is, however, contradictory with the expectations.

The enhancement at low temperature of both hyperfine field and isomer shift at Fe sites (table 1) located in nanocrystalline grains can be interpreted on the basis of a reduced density,

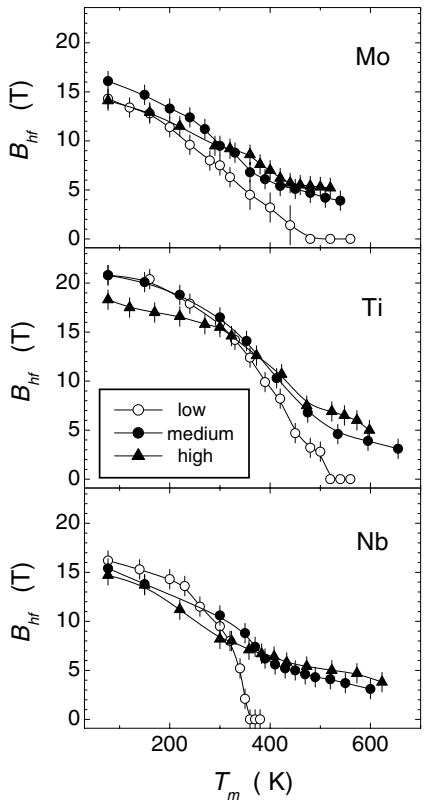

Figure 5. Average hyperfine fields B_{hf} of the amorphous residual phase versus temperature of measurement, T_{m}, for nanocrystalline $Fe_{80}M_7Cu_1B_{12}$ (M = Mo, Nb and Ti) with low, medium and high crystalline fraction.

i.e. an expansion of the lattice parameter. Indeed, the Bethe–Slater curve supports the density reduction of hyperfine field well because it relates the exchange energy to the atomic geometry. In addition, the increase of isomer shift reflects a reduction of electron density at the Fe nucleus. It is important to emphasize that the small variations of hyperfine field and isomer shift are consistent with a weak expansion of the bcc lattice that cannot be evidenced from either XRD or TEM. Its origin might be explained by the introduction of impurities. On the other hand the highest enhancement is due to the smallest atom species (Mo: 1.39 Å) and its rather high diffusivity, in comparison to those of Nb and Ti (atomic radii: 1.46 and 1.47 Å, respectively). Such an effect has to be temperature independent, that is not supported in the present study because the crossover, if any, is observed at around 300 K. In addition, one has to note that a reduction of hyperfine field is observed far above the Curie temperature of the amorphous remainder, even for high crystalline contents (figure 3 (a)). Such a reduction cannot be thus explained by the presence of thermal magnetic fluctuations.

Another explanation assumes the presence of internal stresses induced during the nanocrystallization stage, favouring the presence of expansion and compression of the lattice at low and elevated temperature of measurement, respectively. It is consistent with a slight change of the texture of ferromagnetic domains between 77 and 300 K [29]. One observes a decrease of the intensity of intermediate sextet lines attributed to the crystalline component when the temperature increases as seen e.g. in figure 1. This is in agreement with an in-plane

to an out-of-plane magnetic anisotropy reorientation of the crystalline grains with progressive temperature decoupling of magnetic moments within the amorphous remainder. One suggests thus that nanocrystalline grains undergo extensive internal stresses which progressively turn into compressive internal stresses with increasing temperature, because those nanocrystalline alloys show a positive magnetostriction and because the density within the grains differs from that of the amorphous remainder [30]. It consequently induces some slight changes of lattice parameter of the nanocrystalline grains, thus giving rise to small variations of both hyperfine field and isomer shift values at Fe sites.

At this stage, one can check if such a phenomenon occurs for other nanocrystalline alloys: it is important to emphasize that very few hyperfine data can be collected as a function of temperature, from the literature. Nevertheless, it has already been found in other systems [22, 31, 32]. In addition, the stresses induced during the transformation from the amorphous to the nanocrystalline state are also probably dependent on the amorphicity of the precursor, i.e. its free volume.

5. Conclusion

The temperature behaviour of iron nanograins was investigated in $Fe_{80}M_7Cu_1B_{12}$ Nanoperm-type alloys. Substitution of the metal M by Mo, Nb and Ti revealed differences in magnetic arrangements both in the as-quenched (amorphous) state and after heat treatment when nanocrystallites emerged. The annealing was performed at different temperatures thus providing various amounts of bcc Fe nanocrystalline grains. Consequently, a complexity of hyperfine interactions was studied as a function of the alloy's composition and degree of crystallinity.

The most striking feature of temperature dependences of hyperfine magnetic fields associated with iron nanograins is that they do not follow the same tendency with respect to the composition of the master alloy. For Mo-containing samples, the hyperfine magnetic fields deviate from those of a bulk Fe in the high temperature region proportionally to the contents of nanocrystallites. More pronounced deviations are observed for samples with high nanocrystalline fraction. The opposite trend is evidenced for Nb- and Ti-containing nanocrystalline alloys.

The more probable explanation of the observed effects takes into consideration variations in the density of structurally different regions and subsequently an influence of internal stresses induced in the process of crystallization. Structural modifications thus created are difficult to trace by conventional methods of structural analysis but demonstrate themselves via hyperfine interactions of the affected atoms.

Acknowledgments

Nanocrystalline samples were provided by courtesy of Dr B Idzikowski (Poznan). The work was supported by grant SGA 1/8305/01.

References

[1] Yoshizawa Y, Oguma S and Yamauchi K 1988 *J. Appl. Phys.* **64** 6044–6
[2] Suzuki K, Kataoka N, Inoue A, Makino A and Masumoto T 1990 *Mater. Trans. JIM* **31** 743
[3] Willard M A, Laughlin D E, McHenry M E, Thima D, Sickafus K, Cross J O and Harris V G 1998 *J. Appl. Phys.* **84** 6773–7
[4] Suzuki K, Makino A, Inoue A and Masumoto T 1991 *J. Appl. Phys.* **70** 6232–7

[5] McHenry M E and Laughlin D E 2000 *Acta Mater.* **48** 223–38
[6] Suzuki K 1999 *Mater. Sci. Forum* **312–314** 521
[7] Miglierini M, Kopcewicz M, Idzikowski B, Horváth Z E, Grabias A, Škorvánek I, Dłużewski P and Daróczi Cs S 1999 *J. Appl. Phys.* **85** 1014–25
[8] Kemény T, Kaptás D, Balogh J, Kiss L F, Pusztai T and Vincze I 1999 *J. Phys.: Condens. Matter* **11** 2841–7
[9] Kemény T, Kaptás D, Kiss L F, Pusztai T, Balogh J and Vincze I 2000 *J. Magn. Magn. Mater.* **215/216** 268–71
[10] Suzuki K and Cadogan J M 2000 *J. Appl. Phys.* **87** 7097–9
[11] Hesse J, Hupe O, Hofmeister C E, Bremers H, Chuev M A and Afanas'ev A M 2003 *Materials Research in Atomic Scale by Mössbauer Spectroscopy* ed M Mashlan, M Miglierini and P Schaaf (Dordrecht: Kluwer) pp 117–26
[12] Hupe O, Chuev M A, Bremers H, Hesse J, Afanas'ev A M, Efthimiadis K G and Polychroniadis E K 2003 *Materials Research in Atomic Scale by Mössbauer Spectroscopy* ed M Mashlan, M Miglierini and P Schaaf (Dordrecht: Kluwer) pp 137–46
[13] Hupe O, Chuev M A, Bremers H, Hesse J and Afanas'ev A M 1999 *J. Phys.: Condens. Matter* **11** 10545–56
[14] Idzikowski B, Baszyński J, Škorvánek I, Müller K-H and Eckert D 1998 *J. Magn. Magn. Mater.* **177–181** 941–2
[15] Preston R S, Hanna S S and Heberle J 1962 *Phys. Rev.* **168** 2207
[16] Suzuki K, Cadogan J M, Sahajwalla V, Inoue A and Masumoto T 1996 *Mater. Sci. Forum* **225–227** 707–12
[17] Suzuki K, Cadogan J M, Sahajwalla V, Inoue A and Masumoto T 1997 *Mater. Sci. Eng.* A **226–228** 554–8
[18] Grabias A and Kopcewicz M 1998 *Mater. Sci. Forum* **269–272** 725–30
[19] Grabias A and Kopcewicz M 1999 *Acta Phys. Pol.* A **96** 123–30
[20] Kopcewicz M 1999 *Acta Phys. Pol.* A **96** 49–68
[21] Garitaonandia J S, Gorria P, Fernández Barquín L and Barandiarán J M 2000 *Phys. Rev.* B **61** 6150–5
[22] Miglierini M and Greneche J-M 1997 *J. Phys.: Condens. Matter* **9** 2303–19
[23] Miglierini M, Škorvánek I and Greneche J-M 1998 *J. Phys.: Condens. Matter* **10** 3159–76
[24] Suzuki K and Cadogan J M 1998 *Phys. Rev.* B **58** 2730–9
[25] Brand R A 1987 *Nucl. Instrum. Methods Phys. Res.* B **28** 398–416
[26] Teillet J and Varret F *Mosfit Program* Université du Maine, unpublished
[27] Miglierini M, Seberíni M and Greneche J-M 2001 *Czech. J. Phys.* **51** 677–83
[28] Greneche J-M, Miglierini M and Slawska-Waniewska A 2000 *Hyperfine Interact.* **126** 27–34
[29] Greneche J-M and Varret F 1982 *J. Phys. C: Solid State Phys.* **15** 5333–44
[30] Ok H-N and Morrish A-H 1980 *Phys. Rev.* B **22** 3471–80
[31] Miglierini M and Greneche J-M 1999 *Hyperfine Interact.* **122** 121–8
[32] Škorvánek I, Kovác J and Greneche J-M 2000 *J. Phys.: Condens. Matter* **12** 9085–93